# LONG WAVE PROPAGATION, SHOALING AND RUN-UP IN NEARSHORE AREAS

V.Sriram[1], I. Didenkulova[2,3], S. Schimmels[4], A. Sergeeva[5] and N.Goseberg[6]

This paper discusses the possibility to study propagation, shoaling and run-up of these waves over a slope in a 300-meter long large wave flume (GWK), Hannover. For this purpose long bell-shaped solitary waves (elongated solitons) of different amplitude and the same period of 30 s are generated. Experimental data of long wave propagation in the flume are compared with numerical simulations performed within the fully nonlinear potential flow theory and KdV equations. Shoaling and run-up of waves on different mild slopes is studied hypothetically using nonlinear shallow water theory. Conclusions about the feasibility of using large scale experimental facility (GWK) to study tsunami wave propagation and run-up are made.

*Keywords: long wave dynamics; elongated solitons; propagation; run-up; large-scale experimental facility; numerical simulation*

## INTRODUCTION

For modeling of tsunami wave propagation, shoaling and run-up, often solitary or cnoidal waves have been used (Synolakis 1987). However, solitary and cnoidal-like waves are rarely observed during tsunami propagation. Furthermore, their characteristics are not comparable with most of real–field tsunamis as reported by (Madsen et al. 2008; Goseberg et al. 2013; Schimmels et al. 2014). However, a set of solitary and cnoidal-like waves can be formed in the far field as a result of long wave transformation into an undular bore, as it was observed during 2004 tsunami in the Indian ocean near the coast of Thailand (Fig. 1).

**Figure 1. Indian ocean tsunami of 26 December 2004 approaching Koh Jum island, off the coast of Thailand (Copyright Anders Grawin, 2006).**

Speaking about "typical" tsunami is hard. In reality, the variety of tsunami waves in terms of both periods and wave shapes occur. Due to large-distance propagation and complicated bottom and coastal topography, the initial wave changes its shape, hence, very often even the same tsunami event has very different manifestations at different locations. This is why when talking about tsunami, we should also study different wave shapes.

Based on the past tsunami events, tsunamis approaching the shore may broadly be classified as (e.g. Shuto 1985)

1. Non-breaking waves that act as a rapidly rising tide, observed during small and moderate tsunami events after short distance propagation.
2. Undular bore, observed after tsunami long distance propagation (in terms of wavelength), see Fig. 1.
3. Bore or hydraulic jump (wall of water), observed as a result of wave breaking during large tsunami events after short distance propagation.

Hence, in tsunami studies different types of wave shapes should be considered.

[1] Department of Ocean Engineering, Indian Institute of Technology Madras, Chennai - 600 036, India
[2] Nizhny Novgorod State Technical University n.a. R.E. Alekseev, Nizhny Novgorod 603950, Russia
[3] Institute of Cybernetics, Tallinn University of Technology, Tallinn 12618, Estonia
[4] Forschungszentrum Küste (FZK), Merkurstraße 11, 30419 Hannover, Germany
[5] Institute of Applied Physics, Russian Academy of Sciences, Nizhny Novgorod 603950, Russia
[6] Franzius Institute, Leibniz Universität, Hannover, Germany

It has been demonstrated in (Schimmels et al. 2014) that existing testing facilities with piston type wave makers (with a large stroke) can effectively be used to generate very long non-breaking waves. In this paper we will focus on the possibility to study all the three mentioned types of waves in these facilities.

To do this, a large scale experimental study on generation of long solitary waves with different amplitudes and the same period of 30 s at 1 meter constant water depth has been carried out at the Large Wave Flume (Großer Wellenkanal, GWK) of Forschungszentrum Küste (FZK). Initially, the experimental data of wave propagation are compared with numerical simulations, performed in the framework of fully nonlinear potential flow theory and Korteweg-de Vries (KdV) equations. Later the same waves propagate to the shore and climb "hypothetical" beaches of different slope, confirming that by constructing a mild slope in the Large Wave Flume, one can study the characteristics of tsunami waves of various types.

## NUMERICAL MODELLING

In order to analyze the transformation of long waves during propagation in shallow water depths a numerical wave tank based on fully nonlinear potential flow theory (Sriram et al. 2006) and KdV equations (Sergeeva et al. 2011) is used. In both models the fluid is assumed to be incompressible, the flow is irrotational and viscous forces are neglected.

### Nonlinear potential flow model

The nonlinear potential flow model is based on Laplace's equation for velocity potential $\Phi(x,z)$:

$$\nabla^2\Phi = 0\,, \qquad (1)$$

which is solved in a sub-domain with a wave maker at one end. The computational domain with the corresponding boundary conditions is illustrated in Fig. 2.

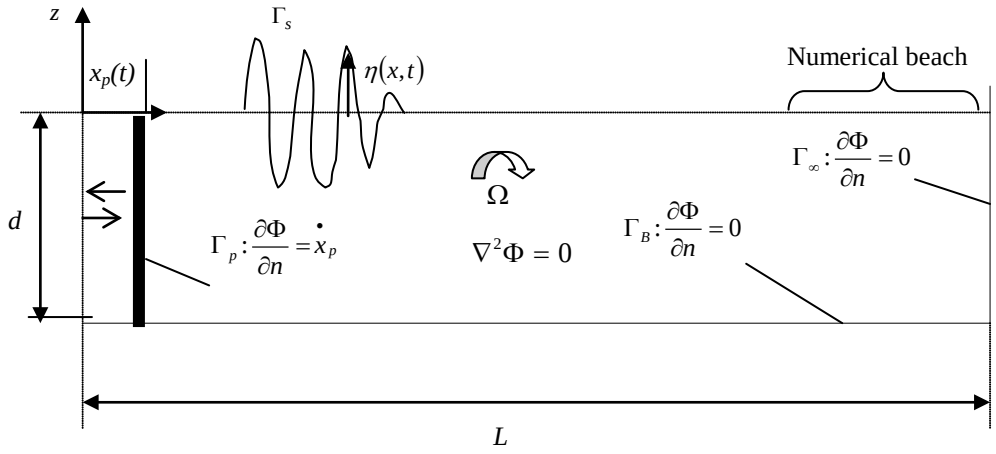


**Figure 2. Numerical representations of the GWK testing facility.**

On the water surface, by considering fully nonlinear terms we can define the kinematic and dynamic free-surface conditions in the Langrangian form:

$$\frac{dx}{dt} = \frac{\partial\Phi}{\partial x}, \qquad \frac{dz}{dt} = \frac{\partial\Phi}{\partial z}, \qquad \frac{d\Phi}{dt} = -g\eta(x,t) + \frac{1}{2}\nabla\Phi\nabla\Phi\,. \qquad (2)$$

The solution for the above boundary value problem (BVP) is sought using a finite element scheme. Formulating the governing Laplace equation constrained with the associated boundary conditions leads to the following finite element systems of equation

$$\int_\Omega \nabla N_i \sum_{j=1}^{m} \phi_j \nabla N_j \, d\Omega\Big|_{j,i\notin\Gamma_s} = -\int_{\Gamma_p} N_i \dot{x}_p(t) d\Gamma - \int_\Omega \nabla N_i \sum_{j=1}^{m} \phi_j \nabla N_j \, d\Omega\Big|_{j\in\Gamma_s, i\notin\Gamma_s}\,, \quad (3)$$

where '*m*' is the total number of nodes in the domain and the potential inside an element $\Phi(x,z)$ can be expressed in terms of its nodal potentials, $\phi_j$, as

$$\Phi(x,z)=\sum_{j=1}^{n}\phi_j N_j(x,z). \qquad (4)$$

Herein, $N_j$ is the shape function and *n* is the number of nodes in an element. The above formulation does not have any singularity effect at the intersection point between the free surface and the boundaries unlike in other methods like BEM. Linear triangular elements with a structured mesh are used. Further details about the numerical model based on finite element method can be referred in (Sriram 2008).

**Korteweg-de Vries equation**

Complimentary to the potential flow model, we use a shallow water model based on the Korteweg-de Vries (KdV) equation (see Sergeeva et al. 2011 for details):

$$\sqrt{gd}\,\frac{\partial\eta}{\partial x}+\frac{3\eta}{2d}\frac{\partial\eta}{\partial s}+\frac{d}{6g}\frac{\partial^3\eta}{\partial s^3}=0\,, \qquad s=\frac{x-x_0}{\sqrt{gd}}-t\,. \qquad (5)$$

Eq. 5 is solved numerically in a periodic domain for *s* with a period *T*. Two integrals of Eq. 5 are conserved:

$$\sqrt{gd}\,\frac{\partial\eta}{\partial x}+\frac{3\eta}{2d}\frac{\partial\eta}{\partial s}+\frac{d}{6g}\frac{\partial^3\eta}{\partial s^3}=0\,, \qquad s=\frac{x-x_0}{\sqrt{gd}}-t\,. \qquad (6)$$

and a pseudo-spectral method for time derivation and a Crank-Nicolson scheme for space discretization are used, see details in Fornberg (1996). The solution of Eq. 5 is calculated in the discrete Fourier space for spectral amplitudes and defined through the Fourier transform $C(\omega) = \mathrm{FFT}\{\eta(s,x)\}$, where the nonlinear part of Eq. 5 is calculated as $C_{non}(\omega) = \mathrm{FFT}\{\eta^2(s,x)/2\}$

$$C(\omega,x+\Delta x)=C(\omega,x-\Delta x)\frac{1+i\beta\omega^3\Delta x}{1-i\beta\omega^3\Delta x}-\frac{3}{2d\sqrt{gd}}\mathrm{FFT}\left\{\frac{1}{2}\eta^2(s,x)\right\}\frac{i\omega\Delta x}{1-i\beta\omega^3\Delta x}\,,\quad \beta=\frac{d^{1/2}}{6g^{3/2}}\,. \qquad (7)$$

**PROPAGATION OF SOLITARY WAVES**

For tsunami propagation analysis we generate solitary waves in the form of elongated solitons, as in Didenkulova et al. (2008)

$$\eta(x,t)=H\,\mathrm{sech}^2\left[k\left(c(t-T)-x\right)\right],\quad k=\frac{2\pi}{cT}\,,\quad c=\sqrt{g(d+H)}\,. \qquad (8)$$

where *H* is the wave amplitude and *T* is its period.

The generation of these long waves is discussed in (Schimmels et al. 2014). The test cases based on these equations are shown in Table 1.

**Table 1. Details of the test cases.**

| Test No. | Depth (m) | Wave period (s) | Wave height (m) |
|---|---|---|---|
| 13/4 | 1.0 | 30 | 0.12 |
| 13/5 | 1.0 | 30 | 0.11 |
| 13/10 | 1.0 | 30 | 0.10 |
| 14/7 | 1.0 | 30 | 0.08 |
| 14/9 | 1.0 | 30 | 0.06 |
| 14/10 | 1.0 | 30 | 0.05 |
| 14/11 | 1.0 | 30 | 0.04 |

In the following we exemplarily consider three cases (14/11, 14/9 and 13/4) representing small, medium and steep waves for detailed analysis. The experimental data as well as KdV and FNPT-FEM simulations are shown in Fig. 3. The corresponding stroke for the above cases is also shown in the figure, demonstrating the increase of required stroke with increasing wave height. Both the FNPT-FEM, KdV models and experimental measurements are in good agreement. The KdV simulations are carried out using the wave time history from FNPT-FEM model at 50 m as initial values.

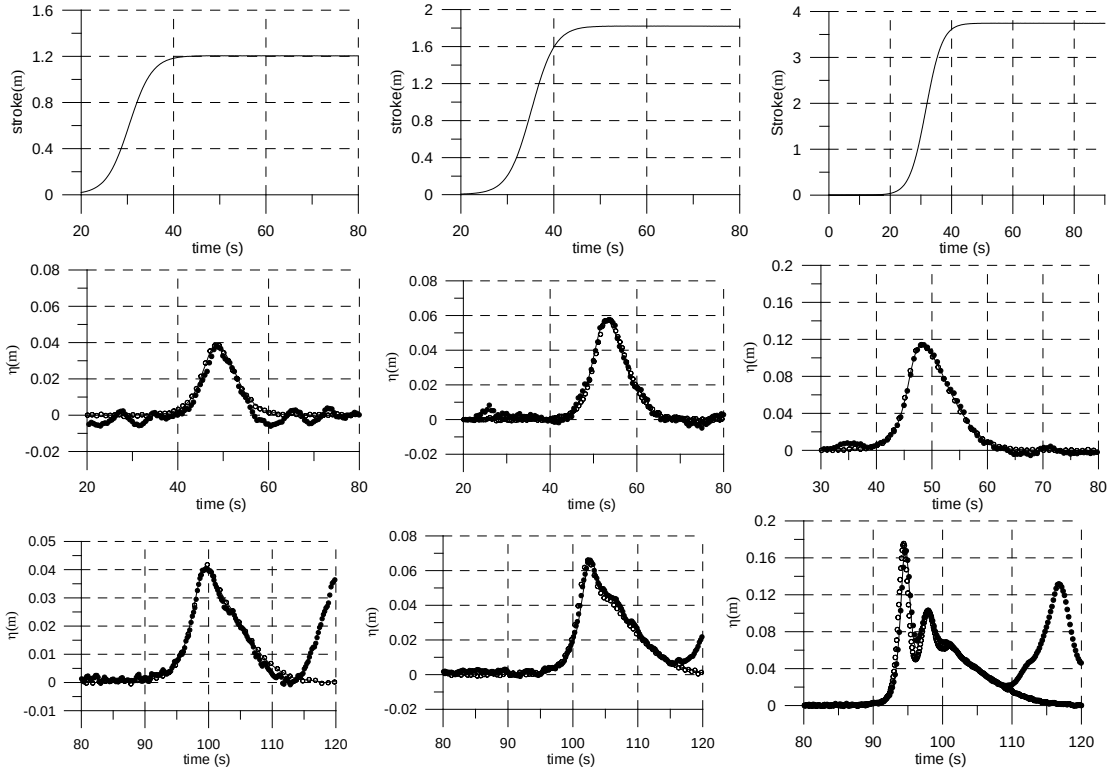


**Figure 3. Comparison between experiments (filed circle), FNPT-FEM simulation (line) and KdV solution (open circle) for positive wave pulses with period of 30 s and amplitudes *H* = 0.04 m (left), 0.06 m (middle) and 0.12 m (right). Top plot: Wave paddle stroke, middle: at *x* = 60 m from the wave paddle; bottom: at *x* = 225 m from the wave paddle.**

It can be seen in Fig. 3 that all waves undergo significant transformation at 225 meter distance, which manifests different dependencies on initial wave amplitude. The smallest 0.04 m wave behaves like a Riemann wave, preserving its amplitude and becoming more asymmetric with a steepening of the face front. The wave of 0.06 m amplitude is more affected by dispersive effects and demonstrates the beginning of the split-up of the initial pulse into Korteweg-de Vries solitons. The beginning of separation of the first soliton is visible in the face front of the wave. A very nice description of this process is given in the paper by Madsen et al. (2008). Finally, the largest 0.12 m wave at the toe of the beach slope progresses much more in the wave separation into solitons, so that three of them can easily be distinguished in the signal. This split-up corresponds to an undular bore formation, which demonstrates the ability of GWK to be an appropriate facility for studying both types of tsunami waves, long nonbreaking surging waves and undular bores (see the classification provided in the Introduction). The second wave that is present in the experiments corresponds to the reflection from the slope.

The distance where the wave starts to split up can be estimated from the nonlinear shallow water theory as the wave breaking distance $X$ (Didenkulova et al. 2006, Zahibo et al. 2008)

$$X = \frac{\sqrt{gd}}{\max\left(-dV/dt\right)}, \qquad V = 3\sqrt{g(d+\eta)} - 2\sqrt{gd}\,. \qquad (9)$$

Estimates based on Eq. 9 are calculated using the time series record at 50 m and are shown in Table 2 (third column) together with the results from the numerical models. The latter were estimated from the water surface elevation time series at different locations as shown in Fig. 4.

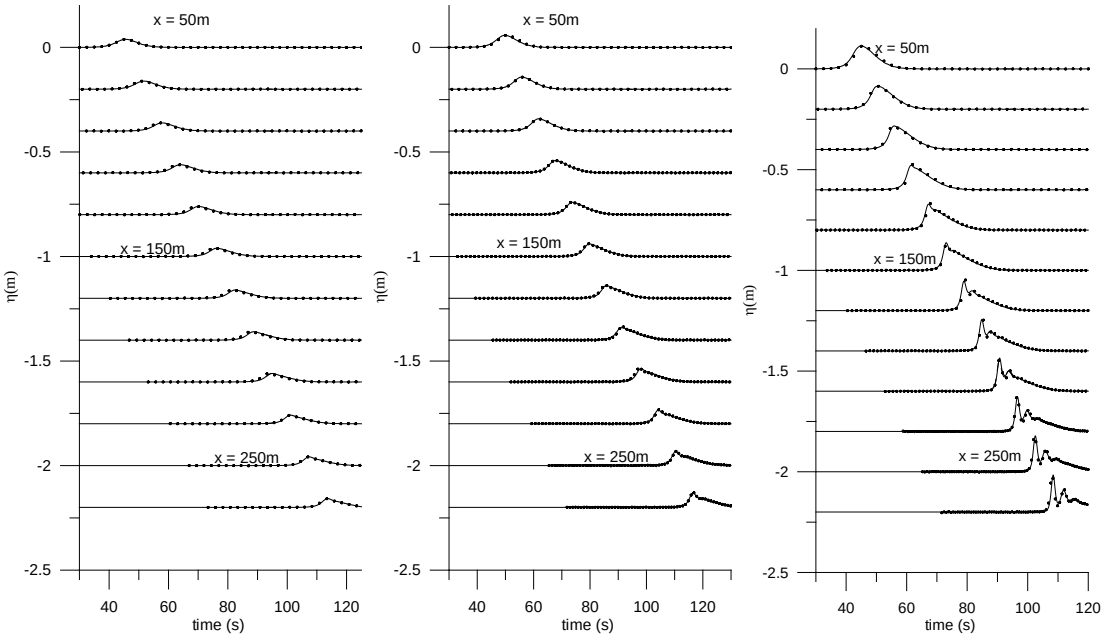


**Figure 4. FNPT-FEM (line) and KdV (dots) simulations of propagation of solitary waves of period 30 s and amplitudes *H* = 0.04 m (left), 0.06 m (middle) and 0.12 m (right). The water surface elevation at different locations shows the splitting of the wave forms.**

**Table 2. Splitting locations from theory (SWT) and numerical simulations (FNPT-FEM and KdV).**

| Test No. | Wave height (m) | SWT (m) | FNPT-FEM (m) | KdV (m) |
|---|---|---|---|---|
| 14/11 | 0.04 | 341 | -- | -- |
| 14/9 | 0.06 | 251 | 250 | 250 |
| 13/4 | 0.12 | 147 | 146 | 146 |

The split up of a long wave into solitons is well-described by KdV equation. For the initial wave described by Eq. 8 the number of formed solitons and their amplitudes can be found from (Pelinovsky 1996)

$$H_n = \frac{H}{4Ur}\left[\sqrt{1+8Ur} - (2n-1)\right]^2 \quad , \quad n = 1, 2, \ldots N, \quad N = \left\lfloor \frac{\sqrt{1+8Ur}+1}{2} \right\rfloor , \qquad (10)$$

where *Ur* is the Ursell number. It can be seen from Eq. 10 that the amplitudes of formed solitons cannot exceed twice amplitude of the initial wave. For example, for a wave with $H$ = 0.12 m, the largest soliton has an amplitude of 0.19 m. This is in agreement with the FNPT-FEM model, wherein the first wave height after 270 m is about 0.185m.

## RUN-UP OF SOLITARY WAVES

It has been shown that the validated numerical model based on FNPT describes wave dynamics very well. However, it is not able to model the wave run-up process. This is why for studying wave run-up on a beach, it is better to use a hybrid FNPT-NS model based on FEM and MLPG_R (Sriram et al. 2014). In the present study, run-up has been studied by means of analytical solutions (Didenkulova 2009) and differently transformed long waves were investigated on different slopes. This approach is much faster than the hybrid FNPT-NS and provides a good preliminary estimate.

The sea surface elevation at the beginning of the slope is used as input to study wave run-up on a beach. Figure 5 shows the corresponding inundation on a 1:6 slope, like in GWK. Apparently the inundation patterns get expectedly more complicated with increasing amplitude of the incident wave and they strongly depend on the wave transformation during propagation along the flume. It can be seen that the inundation length increases nonlinearly with an increase in the initial wave amplitude. This is even more visible in Fig. 6, where the normalized run-up oscillations are displayed. From Fig. 6 one can see that the amplification factor (the ratio of the maximum run-up height to the maximum wave height at the toe of the slope) increases with an increase in the amplitude of the initial pulse. So, the

wave amplification on the beach for the 0.04 m wave is 2.5, for the 0.06 m wave 2.8 and for the 0.12 m wave it is 3.4.

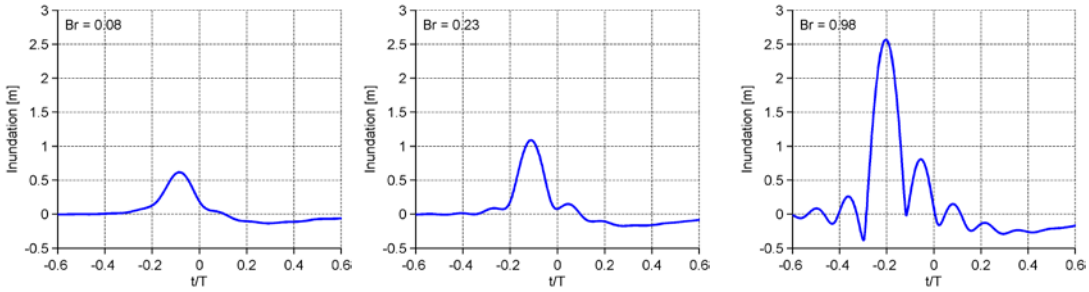


**Figure 5. Inundation of a mild slope of 1:6 by solitary waves with amplitudes *H* = 0.04 m (left), 0.06 m (middle) and 0.12 m (right).**

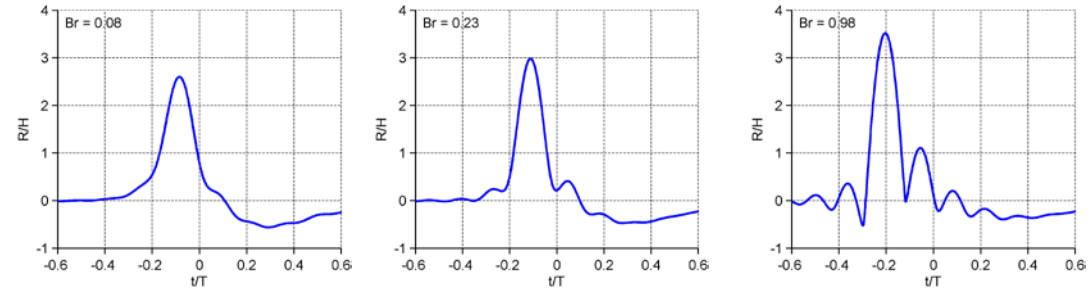


**Figure 6. Normalized run-up height of solitary waves with amplitudes *H* = 0.04 m (left), 0.06 m (middle) and 0.12 m (right) on a mild slope of 1:6.**

The parameter *Br* plotted in Figs. 5 and 6 is the wave breaking parameter:

$$Br = \frac{\max\left(\frac{d^2 r}{dt^2}\right)}{g\alpha^2} \le 1, \qquad (11)$$

which indicates wave breaking during run-up. Here $r$ is the run-up oscillations on the beach and $g$ is the gravity acceleration. If $Br < 1$, the wave is not breaking. For $Br = 1$ the wave experiences first breaking just at the beach. This occurs in the back-wash stage and is manifested by the bubble formation when the water is at its maximal offshore position.

## EFFECT OF THE SLOPE

Analysis of the effect of the beach slope has been studied hypothetically considering the possibility of constructing an artificial slope of different inclinations in GWK. For this we studied propagation of the initial pulse in the basin of constant depth (1 m) and distance $L$ (from the wave generator to the beginning of the slope) and then its run-up on the slope $\alpha$. The propagation was performed using FNPT-FEM, which proved to be good for description of long wave dynamics in GWK. Run-up height was calculated based on nonlinear shallow water theory. Both slope $\alpha$ and distance $L$ have been changing in order to keep the total length of the basin constant (see Fig. 7).

The result of this analysis is shown in Fig. 8 for the initial 0.04 m pulse which climbs three different beach slopes: natural 1:6 GWK slope (blue solid line), 1:12 (red solid line) and 1:17 (green solid line). It can be seen, that the inundation distance increases substantially with a decrease in the beach slope. For example, the difference in inundation distance on 1:6 and 1:17 slopes is almost 70%.

Figure 9 demonstrates how the amplification ratio of the solitary wave on a beach changes with the corresponding change of the beach slope.

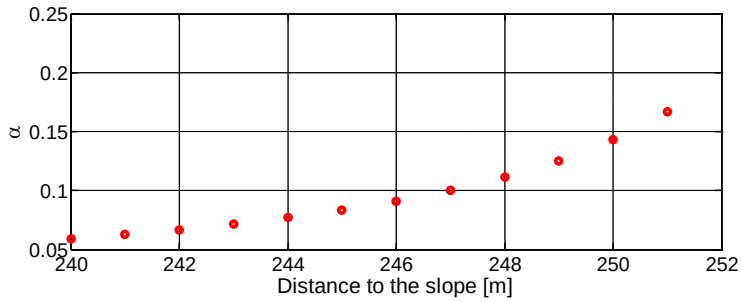


**Figure 7. Beach slope *α* with respect to the distance *L*.**

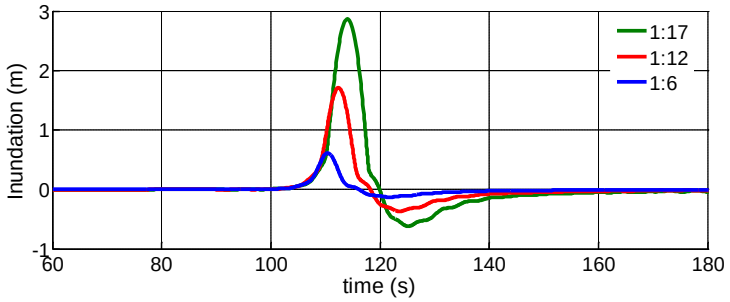


**Figure 8. Inundation of 4 cm high elongated solitary pulse for three types of the beach slope: natural 1:6 slope of GWK (blue solid line), 1:12 (red solid line) and 1:17 (green solid line).**

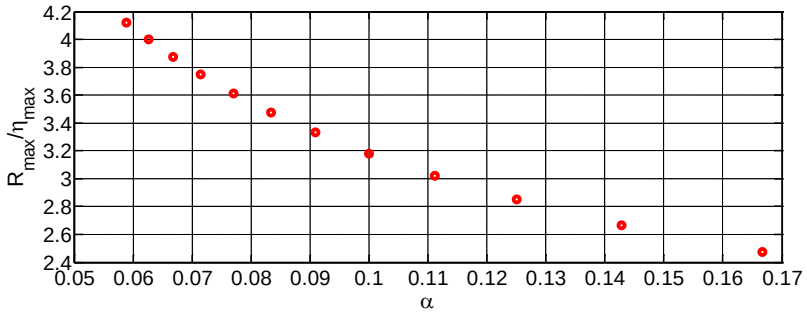


**Figure 9. Amplification ratio of 4 cm wave on a beach with slope *α*.**

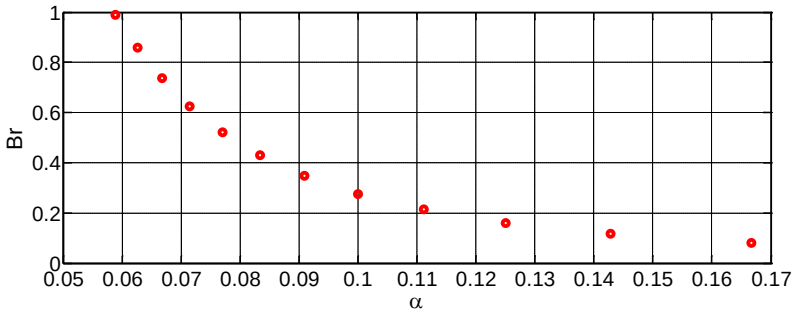


**Figure 10. Breaking parameter for the 4 cm wave on the beach with different slopes *α*.**

With this analysis based on analytical solutions of shallow water theory we are limited to the non-breaking wave propagation and run-up, which corresponds to values of $Br \leq 1$. Behavior of breaking parameter *Br* for 4 cm wave climbing different slopes is shown in Fig. 10. It can be seen that even the 4 cm wave at the slope of 1:17 is already at the point of breaking. The wave of 12 cm will break already at the slope of 1:7 - just a little bit milder than the current GWK slope. For further decrease in the beach slope, the wave will form a steep front with further plunging breaking and bore formation. So, in this way all three types of waves according to the classification of Shuto (1985) can be reproduced in GWK.

## CONCLUSION

The potential of large scale facilities and in particular the 300-meter long Large Wave Flume (GWK) for tsunami wave propagation and run-up has been examined. Three types of long waves: non-breaking surging waves, bore or hydraulic jump and undular bore have been considered for feasibility analysis. By studying the dynamics of long solitary pulses (elongated solitary waves) with different amplitudes and the same period of 30s it has been demonstrated that all three types of waves can be formed at the beach, if different beach slopes are considered. Thus, it can be concluded that the existing test facility in GWK can be used for tsunami research by constructing a mild slope (or bathymetry of a particular area) and investigating the run-up and inundation characteristics.

## ACKNOWLEDGMENT

Dr. V. Sriram and Dr. I. Didenkulova would like to thank Alexander von Humboldt (AvH) foundation for their grants and network meetings. Dr. I. Didenkulova further acknowledges the basic part of the State Contract No 2014/133 and grants MK-1146.2014.5 and SF0140007s11. Dr. A. Sergeeva thanks grants from RFBR (14-02-00983 and 14-05-00092).

## REFERENCES

Didenkulova, I. 2009. New trends in the analytical theory of long sea wave runup, *Applied Wave Mathematics: Selected Topics in Solids, Fluids, and Mathematical Methods*, Springer, 265-296.

Didenkulova, I., E. Pelinovsky, and T. Soomere. 2008. Run-up characteristics of tsunami waves of "unknown" shapes, *Pure and Applied Geophysics*, 165 (11/12), 2249-2264.

Didenkulova, I., N. Zahibo, A. Kurkin, and E. Pelinovsky. 2006. Steepness and spectrum of a nonlinearly deformed wave on shallow waters, *Izvestiya, Atmospheric and Oceanic Physics*, 42 (6), 773-776.

Fornberg, B. 1996. *A practical guide to pseudospectral methods*, Cambridge University Press, New York, 244 p.

Goseberg, N., A. Wurpts, and T. Schlurmann. 2013. Laboratory-scale generation of tsunami and long wave, *Coastal Engineering*, 79, 57-74.

Madsen, P. A., D. R. Fuhrman, and H. A. Schaffer. 2008. On the solitary wave paradigm for tsunamis, *J. Geophys. Res.*, 113, C12012.

Pelinovsky, E. *Hydrodynamics of tsunami waves*, IPF RAN, Gorky, 1996. [in Russian]

Schimmels, S., V.Sriram , I. Didenkulova, and H. Fernández. 2014. On the generation of tsunami in a large scale wave flume, Proceeding ICCE 2014.

Shuto, N. 1985. The Nihonkai-chuubu earthquake tsunami on the north Akita coast, *Coastal Engineering Japan*, JSCE 28, 255-264.

Sergeeva, A., E. Pelinovsky, and T. Talipova. 2011. Nonlinear random wave field in shallow water: variable Korteweg-de Vries framework, *Nat. Hazards Earth Syst. Sci.*, 11, 323-330.

Sriram, V. 2008. Finite Element Simulation of nonlinear free surface waves, *Phd. Thesis, Department of Ocean Engineering*, IIT Madras, India.

Sriram, V., Q.W. Ma., and T. Schlurmann. 2014. A hybrid method for modelling two dimensional non-breaking and breaking waves. *Journal of computational physics*, 272, 429-454.

Sriram, V., S.A. Sannasiraj, and V. Sundar. 2006. Numerical simulation of 2D nonlinear waves using Finite Element with Cubic Spline Approximation, *Journal of Fluids and Structures*, 22 (5), 663-681.

Synolakis, C.E. 1987. The runup of solitary waves, *J. Fluid Mech.*, 185, 523–545

Zahibo, N., I. Didenkulova, A. Kurkin, and E. Pelinovsky. 2008. Steepness and spectrum of nonlinear deformed shallow water wave, *Ocean Engineering*, 35 (1), 47–52.